Talanta 120 (2014) 419–424

Contents lists available at ScienceDirect

Talanta

journal homepage: www.elsevier.com/locate/talanta

Gold nanoparticle amplified optical microfiber evanescent wave absorption biosensor for cancer biomarker detection in serum

Kaiwei Li [a,b], Guigen Liu [a], Yihui Wu [a,*], Peng Hao [a], Wenchao Zhou [a,b], Zhiqiang Zhang [c]

[a] State Key Laboratory of Applied Optics, Changchun Institute of Optics, Fine Mechanics and Physics, Chinese Academy of Sciences, Changchun 130033, PR China

[b] University of Chinese Academy of Sciences, Beijing 100039, PR China

[c] Suzhou Institute of Biomedical Engineering and Technology, Chinese Academy of Sciences, Suzhou 215163, PR China

ARTICLE INFO

Article history:
Received 12 September 2013
Received in revised form
26 November 2013
Accepted 29 November 2013
Available online 6 December 2013

Keywords:
Fiber optic sensor
Optical microfiber
Gold nanoparticle
Cancer biomarker
Alpha-fetoprotein (AFP)

ABSTRACT

Sensitive and selective detection for cancer biomarkers is critical in cancer clinical diagnostics. In this work, we report a new optical microfiber (OMF) biosensor using gold nanoparticles (GNPs) as amplification labels for the detection of alpha-fetoprotein (AFP) in serum samples. By combining the unique optical property of OMFs and the strong optical absorption of GNPs, very high sensitivity and selectivity can be achieved. Critical parameters namely fiber diameter and GNP size were optimized for better performance. The limit of detection (LOD) of this sensor for AFP is 0.2 ng/mL in PBS and 2 ng/mL in bovine serum, which is comparable to conventional assays. The advantages of this biosensor are simple detection scheme, fast response time, and ease of miniaturization, which might make this biosensor a promising platform for clinical cancer diagnosis and prognosis.

1. Introduction

Detection of trace amounts of target proteins in the presence of high concentrations of matrix proteins (e.g., serum samples) is of great significance but remains technically challenging. Existing immunoassays such as fluorescence assay and electrochemiluminescence assay are challenged by their complicated, time-consuming, and labor-intense procedure [1]. Various fiber-optic biosensors (FOBSs) are coming into focus as an alternative to traditional immunoassay owing to their intrinsic advantages such as high sensitivity, fast response time, small footprint, low cost. However, very few of these have been applied in cancer biomarker detection in serum samples due to the strong nonspecific adsorption of sera proteins [2].

Conventional fiber optic fluorescence biosensors possess good selectivity, but their sensitivity is not high enough and suffers from self-quenching [3–5]. Label-free FOBSs based on SPR, LSPR, and fiber gratings can detect subtle index changes caused by the binding of target molecules and can achieve very high sensitivity [6–9]. However, when it comes to clinical samples, the strong nonspecific adsorption of matrix proteins could easily conceal the specific responses, hindering the detection of analytes in crude biological fluids. Several strategies have been developed to increase the specificity of FOBSs. These includes using mixed self-assembled monolayer to suppress nonspecific adsorption [10,11], and using secondary antibody conjugated nanoparticles to enhance the specific response [12,13]. Yet FOBSs used for bioassay in serum samples have seldom been reported. Chang et al. used GNPs to enhance the sensitivity of fiber optic fluorescence biosensors and successfully detected AFP in human serum. However, the problem of self-quenching still remains unsolved [12].

Optical fibers with diameter close to or smaller than the wavelength of light offer a number of favorable properties for optical sensing [14–16]. But their fabrication and packaging are always difficult. Our group has investigated OMF sensors for several years and has made some progress in fabrication and packaging using an on-chip and online etching method [17]. In this work, we developed a simple, highly sensitive, and selective method using OMFs for cancer biomarkers detection in serum. In this OMF biosensor, a sandwich assay strategy was used for the detection by using the biofunctionalized GNPs as the signal amplifier. Compared with multimode fibers, OMFs have a much larger power portion in the evanescent field and several studies have shown that OMFs can realize single nanoparticle detection [18]. Exploiting bioengineered nanomaterials to enhance the performance of biosensors has become a new trend [19,20]. GNPs exhibit strong absorption property in the visible range and have been widely used in many fields, such as sensing, imaging, and solar cells [21–23]. Compared to conventional fluorescent molecules, the optical cross-sections of GNPs are typically 4–5 orders of magnitude higher [24]. In addition, they are photostable and ease in bio-conjugation [25]. By combining the unique

* Corresponding author.
E-mail address: yihuiwu@ciomp.ac.cn (Y. Wu).

0039-9140/$ - see front matter © 2013 Elsevier B.V. All rights reserved.
http://dx.doi.org/10.1016/j.talanta.2013.11.085

optical properties of both OMFs and GNPs, very high sensitivity can be achieved. Moreover, using sandwich assay strategy can also improve the specificity for biodetection in complex media.

α-Fetoprotein (AFP), a well-known tumor marker with a molecular mass of about 68 kDa was chosen as a model protein in biodetection. In healthy human serum, the average concentration of AFP is typically below 25 ng/mL, and an elevated AFP concentration in adult plasma may be an early indication of some cancerous diseases including hepatocellular cancer, yolk sac cancer, and liver metastasis [26]. Using our simple and rapid detection method, AFP could be detected with high sensitivity and selectivity in both phosphate-buffered saline (PBS) and bovine serum.

2. Experimental section

2.1. Reagents and materials

Single-mode optical fiber with core and cladding diameters of 8 μm and 125 μm was purchased from Corning Inc. (New York, USA). Tetrachloro aurate (HAuCl4) and hydrofluoric acid (HF, 40%) were procured from Sinopharm Chemical Reagents Co., Ltd. (Shanghai, China). 3-Aminopropyl-triethoxysilane (APTES, 99%), glutaraldehyde (Grade II, 25% in H2O), phosphate buffer saline (PBS), and bovine serum albumin (BSA) were obtained from Sigma-Aldrich (St. Louis, USA). Two different mouse monoclonal AFP antibodies for different binding sites and AFP antigen were generously supplied from Wondofo Biomedical Co., Ltd (Guangzhou, China). Bovine serum were purchased from Hangzhou Sijiqing Biological Engineering Materials Co., Ltd (Hangzhou China). Polydimethylsioxane (PDMS) was purchased from Dow Corning (Midland, MI, USA). All the reagents were of analytical grade. All solutions were prepared using deionized water (18.2 MΩ cm) obtained from a MilliQ filtration system (Millipore, USA).

2.2. Experimental setup

The experimental setup is shown in Fig. 1A. A white light LED was used as light source and the light was focused into the fiber by a microscope objective. An OMF was fixed in a fluid cell and the cell was integrated with a PDMS chamber for delivery of sample solutions. A home-built spectrometer was used as detector and the data were acquired by a laptop.

2.3. Preparation of OMFs

The preparation of OMFs has been reported in our previous paper [17]. Typically, a length of 10 mm of Corning standard single-mode optical fiber was stripped off the buffer coating and cleaned with acetone. The fiber was then placed in a fluid cell and fixed by PDMS. Afterward, the etching solution was added, and the etching process was monitored by a home-made online monitoring system. The fluid cells were fabricated on silicon chips by MEMS technology and a typical image is depicted in Fig. 1B. The waist diameters of the OMFs can be controlled precisely by monitoring the output power. All the OMF have a waist length of about 6.0 mm because the length of the micro channel is 6.0 mm. A typical OMF with a diameter of 1.0 μm is shown in the inset of Fig. 1B. The fluid cell was then integrated with a PDMS chamber for delivery of sample solutions (Fig. 1C).

2.4. Immobilization of antibodies on the OMF surface

Briefly, the fibers were cleaned for 10 min in a bath consisting of 1 vol of 30% H_2O_2 and 3 vol of concentrated H_2SO_4 to generate reactive hydroxyl groups. The cleaned fiber was then immersed in

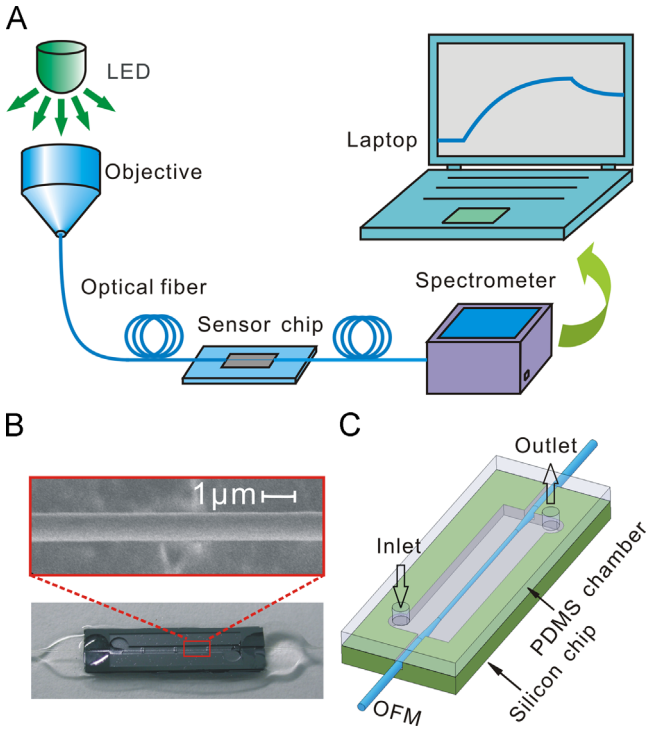

Fig. 1. (A) Illustration of the experimental setup. (B) Image of a sensor cell and SEM image of a 1.0 μm thick optical microfiber. (C) Schematic diagram of an OFM sensor device with an integrated PDMS chamber for sample delivery.

5% solution of APTES in acetone for 2 min and then thoroughly washed with acetone six times and with water for 30 min sequentially [27]. To immobilize antibodies on the fiber surfaces, silanized fibers were first immersed in a 2.5% glutaraldehyde solution for 30 min and thoroughly rinsed with PBS. Afterward, the fibers were immersed in an antibody solution with a concentration of 10 μg/mL at 4° overnight [27]. A solution of 1% BSA in PBS was used to block the unreacted sites to minimize nonspecific adsorption [28].

2.5. Preparation of GNPs and bio-conjugation

The GNPs used in the present study were synthesized following a method introduced by Turkevich [29]. The size of the GNPs was confirmed by SEM images, and the UV–vis absorption spectra were also recorded by a Lambda 850 spectrophotometer. The mole concentration of these GNP solutions was calculated according to the method proposed by Haiss [30]. Antibodies were electrostatically bound to the GNPs following the protocols described by Hermanson [31].

2.6. Detection mechanism of the biosensor

The main mechanism of this biosensor is the selective absorption of evanescent wave by GNPs when they approach the fiber surface. The sandwich assay shown in Fig. 2 was used for the detection of AFP molecules. First antibody was immobilized on the OMF as the capture antibody. Secondary antibody functionalized GNPs were used as signal amplifiers. OMFs exhibit a prominent evanescent field with a depth of about several hundreds nanometers in the surrounding medium [32]. GNPs binding to the surface through specific interaction can induce great losses in the output light due to their remarkable absorption property. Thus, antigens can be detected by this sandwich amplification strategy.

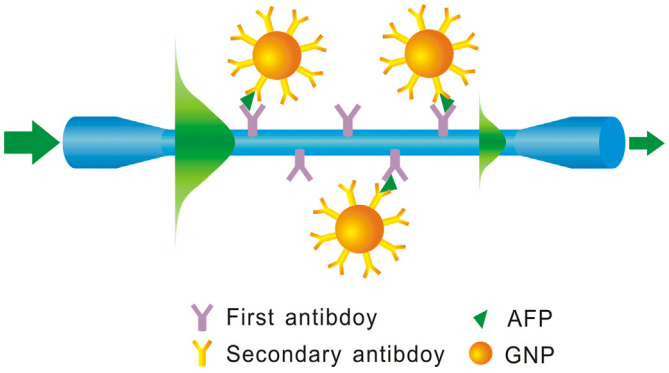

Fig. 2. Schematic diagram of the immunoassay for α-Fetoprotein (AFP) detection using GNPs as signal amplification labels.

3. Results and discussion

3.1. Optimization of the sensing strategy

In order to obtain good performance, the diameter of the OMF and size of GNP were optimized through theoretical calculations combined with experimental considerations. The main underlying detection mechanism of our sensor involves evanescent field absorption and scattering by GNPs. A large fraction of power in the evanescent field is the key point in developing this biosensor. Normally, the evanescent wave exponentially decays as a function of radius of the fiber [33]. Thus, ultrathin OMFs should be used to achieve high sensitivity. Furthermore, the optical cross-section of GNPs also should be optimized to enhance their interaction with the evanescent field. Normally, the scattering is negligible compared with absorption when the GNPs are smaller than 60 nm [24]. Here, we only consider GNPs range from 15 nm to 50 nm. Thus, the fraction of evanescent field outside the fiber core and the absorption ability of the GNPs are the two main factors that determine the sensitivity of the sensor when the length of an OMF is fixed.

We adopted a model we proposed previously with slight modifications [34]. Assume the number of GNPs on the fiber surface of the OMF is n and they are isolated from one another on the fiber surface. Let P and P_0 denote the transmitted power with and without GNPs on fiber surface; thus

$$P = P_0 \exp(-\eta n C_{abs}) \quad (1)$$

where η is the fraction of power in the evanescent field, and C_{abs} is the absorption cross section of a GNP.

The fraction of HE_{11} modal power in the surrounding medium (RI: 1.333) of an OMF (RI: 1.450) at 520 nm wavelength with diameter as the variable is depicted in Fig. 3A. It is clear that the power fraction in the evanescent field increases dramatically as the diameter decreases from 3.5 to 0.5 μm and the transmitted power P will decrease rapidly accordingly. This means the sensitivity for GNPs can be greatly enhanced by thinning the fiber. Obviously, using nanofibers we can obtain ultrahigh sensitivity. However, the fabrication of nanofibers is very difficult, and they are very fragile to handle. Hence, we chose 1.0 μm thick OMFs to perform the immunoassay based on considerations such as easy fabrication and relatively high sensitivity.

The optical properties GNPs can be calculated through Mie theory [35]. Their optical cross-sections are typically 4–5 orders of magnitude higher than that of conventional dyes [24], indicating the feasibility of achieving signal amplification using GNPs. As shown in Fig. 3B, C_{abs} can be greatly enlarged simply by increasing the GNP size, which will induce more power loss to the transmitted power P. Thus, the larger the GNPs are, the more sensitive the senor is. However, consider that large GNPs about 50–100 nm in diameter are difficult to stabilize and

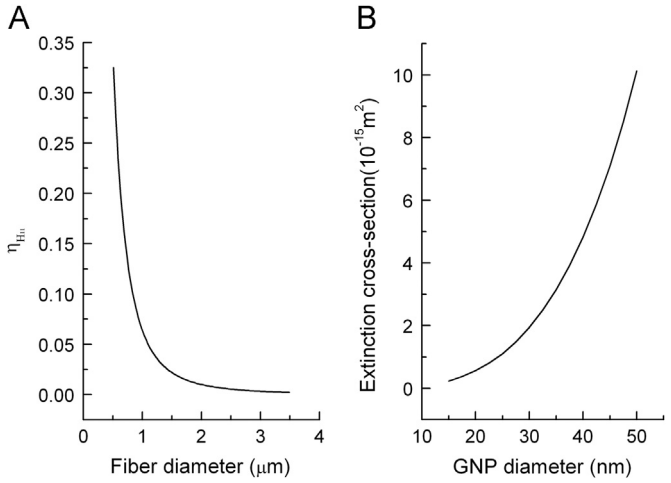

Fig. 3. (A) Fraction of HE_{11} modal power in the external of an OMFs at 520 nm wavelength. The RI of the medium and OMF are 1.333 and 1.450, respectively. (B) Extinction cross-section of gold nanoparticles at the wavelength of their absorption peaks.

can easily aggregate [36]. So GNPs of 40 nm in diameter were used to maintain both high sensitivity and good stability.

3.2. Antibody–GNP conjugation

The binding of antibody to the GNPs occurs by displacement of weakly bound citrate ions on the GNP surface. The optimum conditions required for conjugation and stabilization were determined to be 9 μg for 1 mL of the as prepared GNP solution. As depicted in Fig. 4, spectra analysis of GNPs showed only a slight shift of 5 nm in the wavelength of maximum absorbance following bio-conjugation. This red shift resulted from the formation of a dielectric monolayer of protein around GNPs. This antibody functionalized GNPs solution can be stored in the dark at 4 °C for several months with no signs of aggregation.

Prior to the sandwich assay, the antibody functionalized GNPs solution was tested by an AFP coated OMF. An obvious decline in the spectra was observed immediately after the injection of antibody functionalized GNPs solution. This demonstrated the reactivity of the biofunctionalized GNPs to AFP molecules. Representative absorption spectra are plotted in the inset of Fig. 4. The spectra are analogous with the absorption spectra of GNPs solutions and have an absorption peak at 523 nm, indicating that the power loss was mainly caused by the absorption of GNPs. This was also confirmed by a SEM image shown in the inset of Fig. 4. Thus, 532 nm was used as the detection wavelength to achieve the best sensitivity.

3.3. Detection of AFP in PBS buffer

To fully explore the potential of this ultrasensitive sensor, a systematic study was carried out by detecting AFP in PBS buffer. AFP binding was performed by injecting 100 μl of AFP solution in PBS buffer with concentrations ranging from 0.2 to 1000 ng/mL and incubating at room temperature for 15 min. For further amplifying the biding reaction, 100 μl of 1% (v/v) secondary antibody functionalized GNPs solution diluted in 0.25% BSA solution was injected and incubated for 15 min. The sensorgrams are depicted in Fig. 5A. While there was no distinguishable response observed when AFP binds to the fiber surface, the absorption signal significantly increased when the secondary antibody–GNPs complex were injected. This indicated that GNPs were bond to the OMF surface though specific interactions and the increase in absorption signal was mainly caused by the evanescent power loss induced by strong optical absorption of those GNPs that came into the evanescent

field. Clearly, the employment of the secondary antibody–GNPs complex greatly enhanced the binding signal. The sandwich assay with GNPs enabled the detection of AFP levels as low as 0.2 ng/mL, supporting its utility to assay clinical relevant AFP concentrations. Fig.5B illustrates the calibration curve (black curve) for different AFP concentrations ranging from 0.2 to 1000 ng/mL. Obviously, the detection of low AFP concentrations benefits more from the introduction of the gold enhancement step. Steric hindrance is possible explanations for the limited enhancement for higher concentrations of AFP.

Specificity is an important characteristic for biosensors. To ensure that the enhanced AFP detection is specific, a control measurement namely injection of 1% (v/v) secondary antibody functionalized GNPs solution in the absence of AFP was carried out. The response curve alongside the response curve for the detection of 0.2 ng/mL AFP is displayed in Fig. 5C. It is clear from control experiment that the nonspecific adsorption of the secondary antibody–GNPs complex was negligible and the response signals for different concentrations of AFP were from specific interactions. Thus we can establish 0.2 ng/mL as the LOD for AFP in PBS buffer.

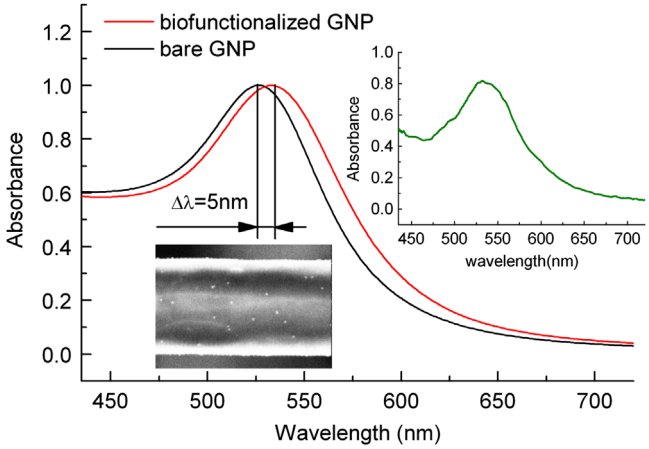

Fig. 4. Absorption spectra of GNP solution and biofunctionalized GNP solution with diameter of 40 nm measured by Lambda 850. The insets show the absorption spectra of the secondary antibody functionalized GNPs binding to an AFP coated OMF sensor and a SEM image of the fiber decorated with GNPs.

3.4. Detection of AFP in bovine serum

There is a significant difference in the limit of detection when clinical samples (serum) are used as the assay media. This change in the detection limit is mainly due to lower signal to noise ratio resulting from high nonspecific adsorption of sera proteins to the sensor surface. This is especially noticeable when label-free biosensors are employed. In the current study, we first investigated the nonspecific adsorption of bovine serum proteins on an OMF sensor surface. As shown in Fig. 6A, when bovine serum was injected, a fast increase in the absorbance signal was observed, which is mainly caused by the nonspecific adsorption of sera proteins. This response is much larger than the specific response of 1 μg/mL AFP in PBS buffer. This may to some extend undermine the performance of our sensor.

Finally, to demonstrate the feasibility of this sensing strategy for clinical applications, bovine serum samples spiked with different concentrations of AFP ranging between 0.2 and 1000 ng/mL was tested using the sandwich assay. Real-time response curves are displayed in Fig. 6B, from which; we can see that the sensor response to the 0.2 ng/mL AFP sample could not be distinguished from the baseline. This may be attributed to the presence of a high level nonspecific adsorption of sera protein. However, the response for a concentration of 2 ng/mL could be distinguished clearly. And this concentration could be determined as the LOD for AFP samples in bovine serum. A calibration curve is shown in Fig. 6C.

Compared with the calibration curve of assay in PBS, it is obvious that the absorbance response in bovine serum was lower. Possible explanations may lie in two aspects: (a) the massive nonspecific adsorption of sera proteins to the sensor surface may cover some of the first antibody and reduce the activity of the sensing surface; (b) the presence of high concentration of sera protein in the media can hinder the mobility of AFP molecules and few AFP are accessible to the sensor surface. Even though, these results show that this OFBS with GNP signal amplification have great potential for the rapid and sensitive detection of tumor biomarkers in clinical samples. Compared with other immunosensors such as fluorometry and enzyme-linked immunoassay, which need complex and time consuming procedures, our sensor

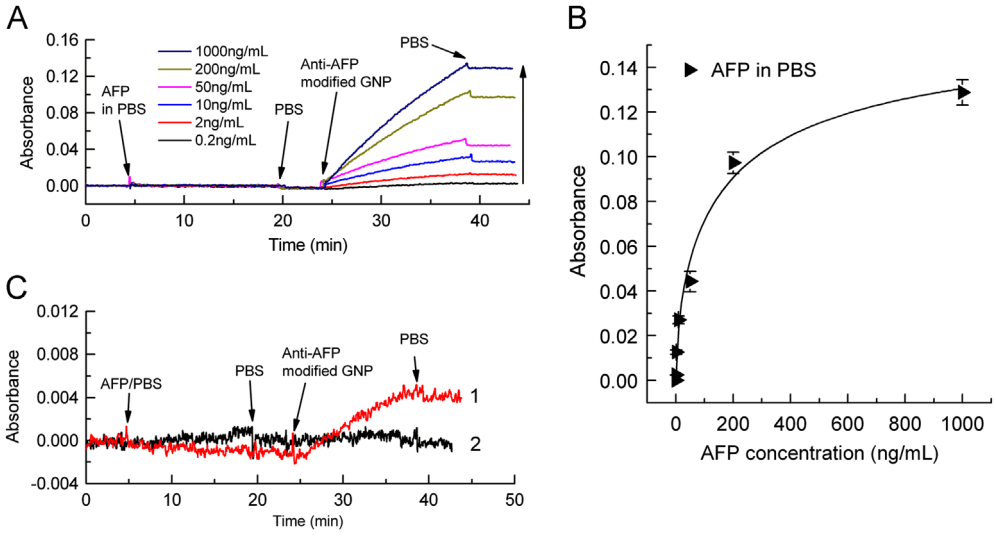

Fig. 5. (A) Absorbance response of a 1.0 μm OMF to different AFP concentrations in PBS buffer using sandwich assays. (B) Calibration curve of the biosensor as a function of analyte target concentration in PBS. (C) Control experiments: curve 1 represents injection of 1% (v/v) secondary antibody functionalized GNPs solution in the presence of 0.2 ng/mL AFP; curve 2 represents injection of 1% (v/v) secondary antibody functionalized GNPs solution in the absence of AFP.

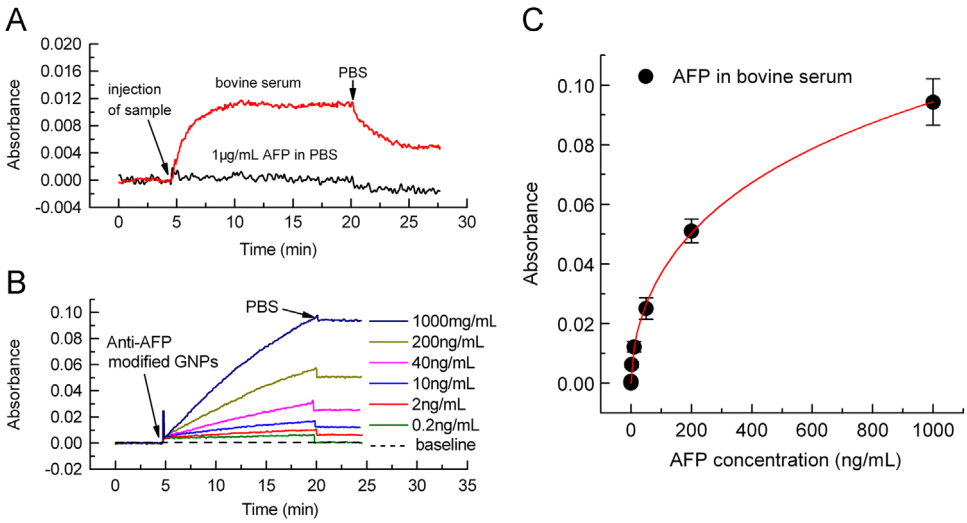

Fig. 6. (A) Absorbance responses of the OMF sensor to 1 μg/mL AFP in PBS and bovine serum without AFP, respectively. (B) Secondary antibody functionalized GNP enhanced sensor response to bovine serum samples spiked with different concentrations of AFP. (C) Calibration curve of the biosensor as a function of analyte target concentration in bovine serum.

has the advantage of simple detection scheme, fast response time and ease of miniaturization [37,38]. In addition, GNPs are photostable and ease in bio-conjugation [25].

3.5. Regeneration of the sensor

Regeneration and reusability are important characteristics for biosensors. To investigate the regeneration of the FOBS, real-time monitoring of AFP functionalized GNP binding to a first antibody functionalized OMF was conducted, and a mild regeneration reagent of 0.1 M glycine–HCl buffer (pH 2.3) was used to dissociate the captured AFP-GNP complex. After each immune response, the regeneration step was carried out by short injections of the regeneration buffer with 1–3 min pulse. As recorded in Fig 7A, the resonance absorbance returned to the initial level after each regeneration cycle. Fig. 7B shows that the sensor can be reused for at least 10 cycles without significant losses in sensitivity.

4. Conclusions

In this work, an evanescent wave-absorption fiber-optic biosensor that combines both the merits of OMF and GNPs was proposed and used for cancer biomarker detection. Theoretical calculations indicated that only when the fiber diameter approaches the order of wavelength could GNPs be readily detected. The sensitivity could be enhanced by decrease the diameter of microfiber or increase the size of GNPs. In the immunoassay, an OMF of 1 μm thick and GNPs of 40 nm are chosen for better sensing performance based on comprehensive considerations. By using secondary antibody functionalized GNPs, the sensitivity and selectivity were greatly enhanced and clinical relevant concentrations of AFP in PBS and a LOD of 0.2 ng/mL was achieved. For complex media, different concentrations of AFP spiked in bovine serum were measured using this sandwich assay and a LOD of 2 ng/mL was achieved. Small foot print, fast response time, repeated usability, and ability to detect AFP in high serum concentrations of the FOBS enable this assay format a promising tool for clinical cancer diagnosis and prognosis.

Yet, the parameters in our experiments were not optimal for achieving highest sensitivity. Some new properties may arise when the fiber diameter goes below 1 μm and ultrahigh sensitivity may be obtained. In addition, various other nanomaterials could also be employed to further improve the performance.

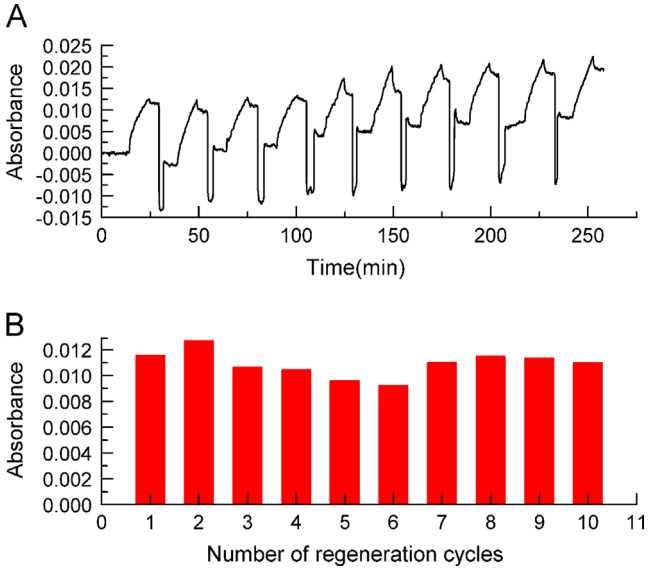

Fig. 7. (A) Real-time response curves for the sensor after a number of regeneration cycles. (B) The sum-up of sensor response for each cycle with background signal subtracted.

Acknowledgments

This study was supported by the Natural Science Foundation of China (11034007, 61102023), the National High Technology Development Program (2012AA040503) and the Technology Development Program of Jilin province. And all the authors express their deep thanks.

References

[1] R. Duan, X. Zhou, D. Xing, Anal. Chem. 82 (2010) 3099–3103.
[2] K.S. Phillips, J.H. Han, Q. Cheng, Anal. Chem. 79 (2007) 899–907.
[3] Y. Wang, W.-H. Liu, K.-M. Wang, G.-L. Shen, R.-Q. Yu, A. Bartlett, Talanta 74 (1998) 33–42.
[4] P.J. Wiejata, P.M. Shankar, R. Mutharasan, Sens. Actuators B Chem. 96 (2003) 315–320.
[5] S.R. Garden, G.J. Doellgast, K.S. Killham, N.J.C. Strachan, Biosens. Bioelectron. 19 (2004) 737–740.

[6] S.-F. Cheng, L.-K. Chau, Anal. Chem. 75 (2003) 16–22.
[7] R. Slavík, J. Homola, E. Brynda, Biosensors and Bioelectronics 17 (2002) 591–605.
[8] Z. He, F. Tian, Y. Zhu, N. Lavlinskaia, H. Du, Biosens. Bioelectron. 26 (2011) 4774–4778.
[9] J.-F. Masson, L. Obando, S. Beaudoin, K. Booksh, Talanta 62 (2004) 865–870.
[10] C.-Y. Chiang, M.-L. Hsieh, K.-W. Huang, L.-K. Chau, C.-M. Chang, S.-R. Lyu, Biosens. Bioelectron. 26 (2010) 1036–1042.
[11] Y.-C.i. Huang, C.-Y. Chiang, C.-H. Li, T.-C.o. Chang, C.g.-S. Chiang, L.-K. Chau, K.-W. Huang, C.-W. Wu, S.-C.u. Wang, S.-R.e. Lyu, Analyst 10 (2013) 1039–1047.
[12] Y.-F. Chang, R.-C. Chen, Y.-J. Lee, S.-C. Chao, L.-C. Su, Y.-C. Li, C. Chou, Biosens. Bioelectron. 24 (2009) 1610–1614.
[13] J. Pollet, F. Delport, K.P.F. Janssen, D.T. Tran, J. Wouters, T. Verbiest, J. Lammertyn, Talanta 83 (2011) 1436–1442.
[14] L. Tong, F. Zi, X. Guo, J. Lou, Opt. Commun. 285 (2012) 4641–4647.
[15] D. Monzón-Hernández, D. Luna-Moreno, D.M. Escobar, J. Villatoro, Sens. Actuators B Chem. 151 (2010) 219–222.
[16] P. Wang, Y. Wang, L. Tong, Light: Sci. Appl. 2 (2013) 1–10.
[17] Y. Wu, X. Deng, F. Li, X. Zhuang, Sens. Actuators B Chem. 122 (2007) 127–134.
[18] J. Zhu, Ş.K. Özdemir, LanYang, IEEE Photon. Technol. Lett. 23 (2011) 1346–1348.
[19] A. Tiwari, A. Tiwari, Bioengineered Nanomaterials, CRC Press, USA, 2013.
[20] A. Tiwari, A.K. Mishra, H. Kobayashi, A.P.F. Turner, Intelligent Nanomaterials, Wiley-Scrivener Publishing LLC, USA, 2012.
[21] S. Zeng, K.-T. Yong, I.t. Roy, X.-Q. Dinh, X. Yu, F. Luan, Plasmonics 6 (2011) 491–506.
[22] R. Popovtzer, A. Agrawal, N.A. Kotov, A. Popovtzer, J. Balter, T.E. Carey, R. Kopelman, Nano Lett. 8 (2008) 4593–4597.
[23] Y.-H. Su, Y.-F. Ke, S.-L. Cai, Q.-Y. Yao, Light: Sci. Appl. 1 (2012) 1–6.
[24] P.K. Jain, Kyeong Seok Lee, I.H. El-Sayed, M.A. El-Sayed, J. Phys. Chem. B 110 (2006) 7238–7249.
[25] A. Gaiduk, P.V. Ruijgrok, M. Yorulmaz, M. Orrit, Phys. Chem. Chem. Phys. 13 (2011) 149–153.
[26] Y. Tamura, S. Yamagiwa, Y. Aoki, S. Kurita, T. Suda, S. Ohkoshi, M. Nomoto, Y. Aoyagi, Dig. Dis. Sci. 54 (2009) 2530–2537.
[27] T. Cass, F.S. Ligler, Immobilized Biomolecules in Analysis: A practical approach, Oxford University Press, 1998, pp. 1–14.
[28] Y.L. Jeyachandran, J.A. Mielczarski, E. Mielczarski, B. Rai, J. Colloid Interface Sci. 341 (2010) 136–143.
[29] S. Link, M.A. El-Sayed, J. Phys. Chem. B 103 (1999) 4212–4218.
[30] W. Haiss, N.T.K. Thanh, J. Aveyard, D.G. Fernig, Anal. Chem. 79 (2007) 4215–4222.
[31] G.T. Hermanson, Bioconjugate techniques, Academic Press, Inc, 1996, pp. 594–605.
[32] A. Leung, P.M. Shankar, R. Mutharasan, Sens. Actuators B Chem. 125 (2007) 688–704.
[33] W. Love, L. Button, R. Slovacek, Optical Characteristics of Fiber Optic Evanescent Wave Sensors, Humana Press, Wise, Wingard (1991) 139.
[34] G. Liu, Y. Wu, K. Li, P. Hao, P. Zhang, M. Xuan, IEEE Photon. Technol. Lett. 24 (2012) 658–661.
[35] C.F. Bohren, D.R. Huffman, Absorption and Scattering of Light by Small Particles, John Wiley & Sons, Inc, 1983, pp. 135–143.
[36] X. Liu, H. Huang, Q. Jin, J. Ji, Langmuir 27 (2011).
[37] Z. Ye, M. Tan, G. Wang, J. Yuan, Talanta 65 (2005) 206–210.
[38] Z. Qiang, R. Yuan, Y. Chai, N. Wang, Y. Zhuo, Y. Zhang, X. Li, Electrochim. Acta 51 (2006) 3763–3768.